Inorganic Chemistry

ARTICLE

pubs.acs.org/IC

Water Attack Umpolung Aromatic Systems To Release Hydrogen

Tsun-Ren Chen,*[†] Hsiu-Pen Lee,[†] and Jhy-Der Chen[‡]

[†]Department of Chemical Biology, National Pingtung University of Education, Pingtung, Taiwan 90003, Republic of China
[‡]Department of Chemistry, Chung-Yuan Christian University, Chung-Li, Taiwan 32023, Republic of China

Supporting Information

ABSTRACT: The synthesis and structures of a series of cyclometalated iridium(III) complexes based on benzoxazole derivatives and triphenylphospine are reported. These complexes have a general formula $(C^\wedge N)_2Ir(Cl)(pph_3)$ [where $C^\wedge N$ is a monoanionic cyclometalating ligand, dfpbo = (difluorophenyl)benzoxazolato, pbo = 2-phenylbenzoxazolato, nbo = 2-(2-naphthyl)benzoxazolato, and pph_3 is a triphenylphospine ligand]. The complexes $(dfpbo)_2Ir(Cl)(pph_3)$ (**2a**), $(pbo)_2Ir(Cl)(pph_3)$ (**2b**), and $(nbo)_2Ir$ $(Cl)(pph_3)$ (**2c**) have been structurally characterized by X-ray crystallography. Complex **2a** shows facile umpolung in the phenyl rings of the arylphosphine ligand and displays a catalytic propensity for water splitting.

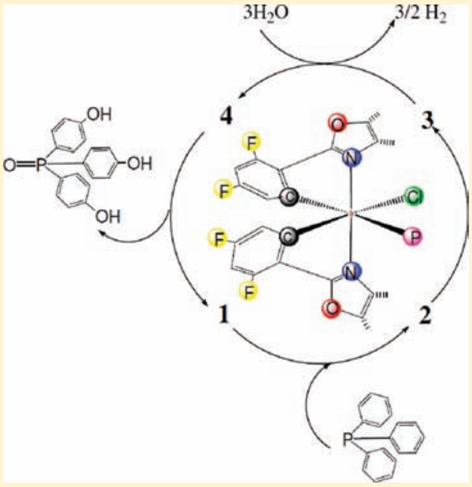

INTRODUCTION

Umpolung, a method for reversing polarity, is one of the most useful strategies for the synthesis of organic or pharmaceutical target molecules.[1] Umpolung for an aromatic system could provide an alternative approach to preparing useful aromatic derivatives or enabling degradation of aromatic pollutants. The umpolung of the aromatic structure has been observed for chromium, molybdenum, and tungsten complexes.[2] However, because of the inertness of these aromatic systems, a strong nucleophile, such as sodium alkoxide, must be used to induce reaction. During our investigation on iridium chemistry, we discovered a new type of iridium complex, which shows facile umpolung in the benzene rings of the arylphosphine ligand, and this complex displays a catalytic propensity for water splitting to produce hydrogen. Hydrogen is a renewable clean energy from a sustainable source, and several kinds of techniques for hydrogen production from the reduction of water have been widely examined, for example, photosynthetic methods by use of semiconductor-based devices and transition-metal complexes in heterogeneous[3] or homogeneous systems.[4] While some of these methods have excellent performance,[4b,c] some were quite complicated.[4d,e] In this paper, we report a new approach to splitting water to release hydrogen.

RESULTS AND DISCUSSION

When iridium dimers $[(C^\wedge N)_2Ir(\mu\text{-}Cl)]_2$ ($C^\wedge N$ = 2-(3.5-difluorophenyl)benzoxazolato-N,C^2 (**1a**), 2-phenylbenzoxazolato-N,C^2 (**1b**), and 2-(2-naphthyl)benzoxazolato-N,C^2 (**1c**)[5] were treated with triphenylphosphine (PPh_3), compounds **2a**−**2c** were obtained (Figure 1). All of these compounds possess a distorted-octahedral coordination geometry and adopt *cis*-N−N chelate disposition (Figures S1−S3 and Tables S1 and S2 in the Supporting Information, SI). Among these three compounds, complex **2a** has the largest C−Ir−N bond angle (designated as α in Figure 2 and Table 1) and also the smallest bond angle N−Ir−P (β). The cyclometalating ligand ($C^\wedge N$) of **2a** is slightly bulkier than that of **2b** but much less bulky than that of **2c**, implying that expansion of the bond angle α for **2a** is due to not only steric repulsion between $C^\wedge N$ ligands but also the electronic effect of the ligands.

To further investigate the effect of the ligand $C^\wedge N$ on the molecular structures, calculations based on density functional theory (DFT; the B3LYP/LANL2DZ level) for **2a**−**2c** were performed.[6] For compound **2a**, the highest occupied molecular orbital (HOMO) is composed of 92% $\pi(C^\wedge N)$ + 5% $\pi(PPh_3)$ + 2% d(Ir) and the lowest unoccupied orbital (LUMO) is composed of 94% $\pi(C^\wedge N)$ + 3% $\pi(PPh_3)$ + 3% d(Ir). For compound **2b**, the HOMO is composed of 81% $\pi(C^\wedge N)$ + 14% $\pi(PPh_3)$ + 3% d(Ir) and the LUMO is composed of 84% $\pi(C^\wedge N)$ + 14% $\pi(PPh_3)$ + 1% d(Ir). For compound **2c**, the HOMO is composed of 92% $\pi(C^\wedge N)$ + 6% $\pi(PPh_3)$ + 1%

Received: December 31, 2010
Published: March 11, 2011

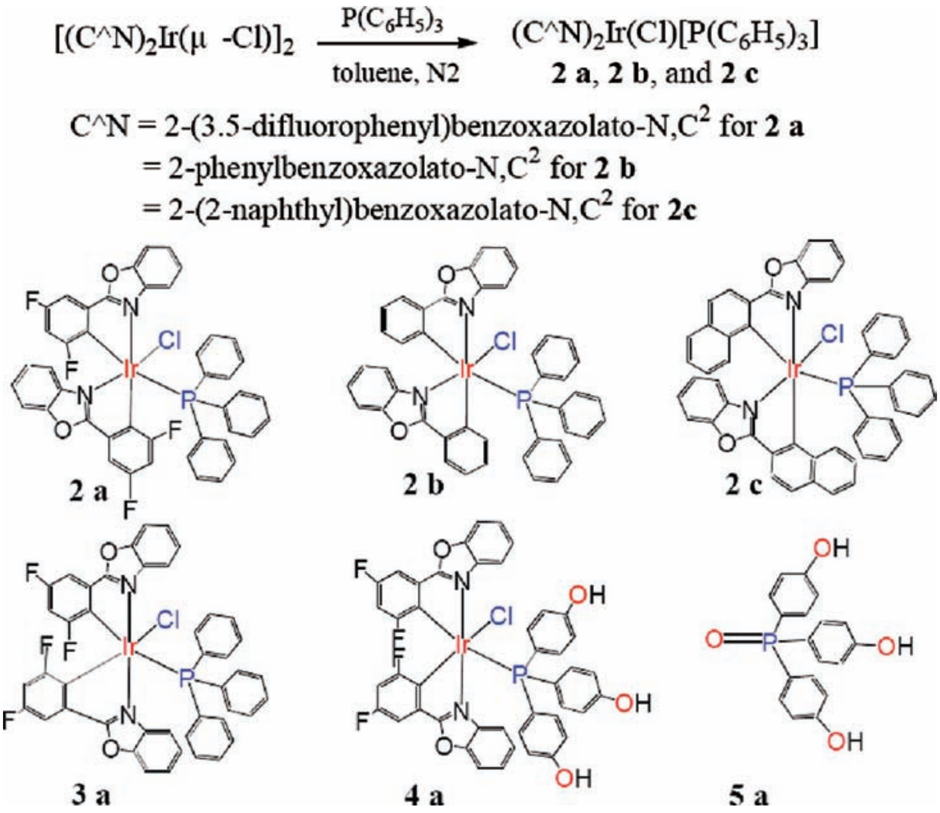

Figure 1. Preparation and molecular structures of **2a**−**2c** and molecular structures of **3a**, **4a**, and **5a**.

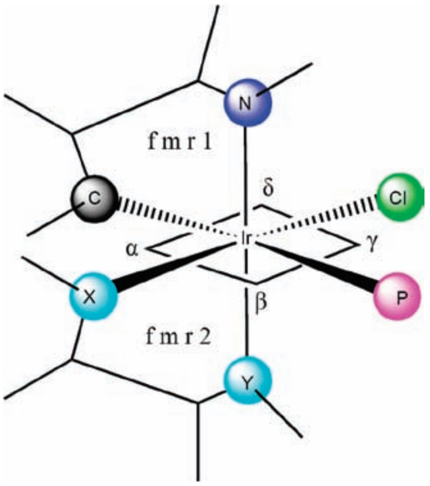

Figure 2. Representation of the bonding configurations for complexes **2a**−**2c** and **3a**, the four bond angles α, β, γ, and δ, and two five-membered rings, fmr1 and fmr2, where X = N and Y = C for **2a**−**2c** and X = C and Y = N for **3a**.

d(Ir) and the LUMO is composed of 86% π(C^N) + 12% π(PPh_3) + 1% d(Ir) (Figure 3 and Figures S4−S6 and Tables S3−S8 in the SI). The calculated dipole moment is 12.94 D for **2a** ($X = -6.8507$, $Y = -7.3126$, and $Z = 8.1917$), 8.80 D for **2b** ($X = -3.13$, $Y = -4.78$, and $Z = 6.70$), and 9.22 D for **2c** ($X = -5.65$, $Y = -2.86$, and $Z = 6.71$). The Mulliken charge distributions show negative charges for the cyclometalating ligands of **2a**−**2c**, which are −1.59, −1.10, and −1.28, respectively, while they show positive charges, +0.78, +0.41, and +0.52, respectively, for the PPh_3 ligands (Figures S7−S9 and Tables S9−S11 in the SI).[7]

Table 1. Some Bonding Parameters for Complexes 2a−2c and 3a

	bond angle (degree)					
cmpd	α	β	γ	δ	md[a] (Å)	DA[b] (deg)
2a	93.50	90.70	90.40	85.30	0.058	79.9
2b	88.67	96.05	89.37	85.91	0.018	90.6
2c	87.42	98.43	87.47	86.43	0.009	93.5
3a	86.33	97.01	92.05	84.64	0.023	86.8

[a] md: average mean deviation from the plane for two five-membered rings, fmr1 and fmr2. [b] DA: dihedral angle between fmr1 and fmr2.

The calculation reveals that all of these three compounds are highly polarized. Most of their electrons are distributed over cyclometalating ligands, and the PPh_3 ligands have a deficiency of electron density. The intramolecular charge interaction involving the electron repulsion between two C^N ligands and the attraction between one of the C^N ligands and the PPh_3 ligand is most obvious for **2a**, which gives rise to not only the largest α and the smallest β for **2a** but also the distortion of two five-membered rings, fmrs. The average mean deviation from the plane of fmrs for **2a** (md = 0.058) is larger than those of **2b** and **2c** (0.018 and 0.009, respectively; Table1). Moreover, this intramolecular charge interaction also makes the octahedral coordination geometry of **2a** very distorted (DA = 79.9 in Table1) and unstable. In the reaction of **1a** with PPh_3, the intermediate **2a**

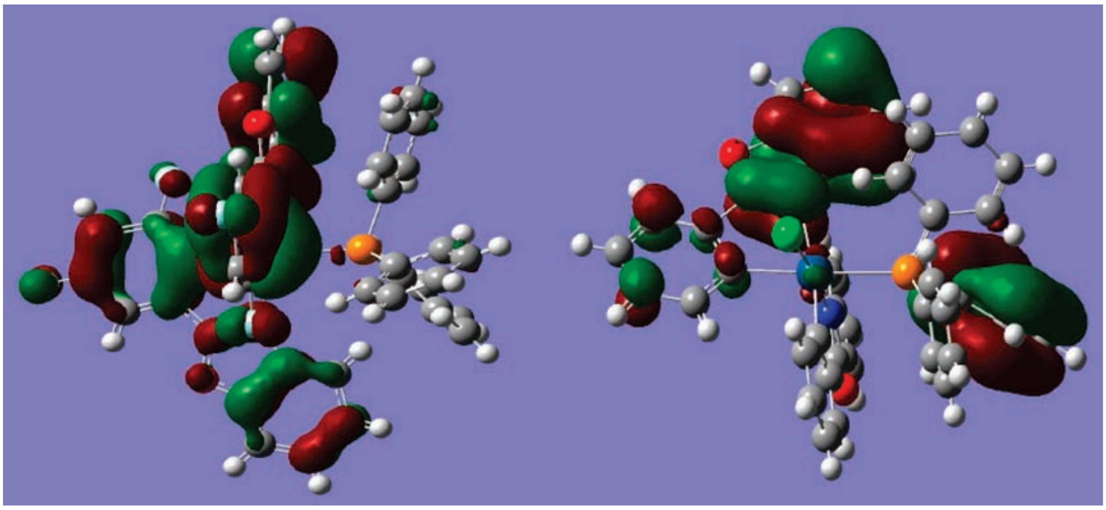

Figure 3. Electron density of the HOMO of **2a** (left) and **2b** (right).

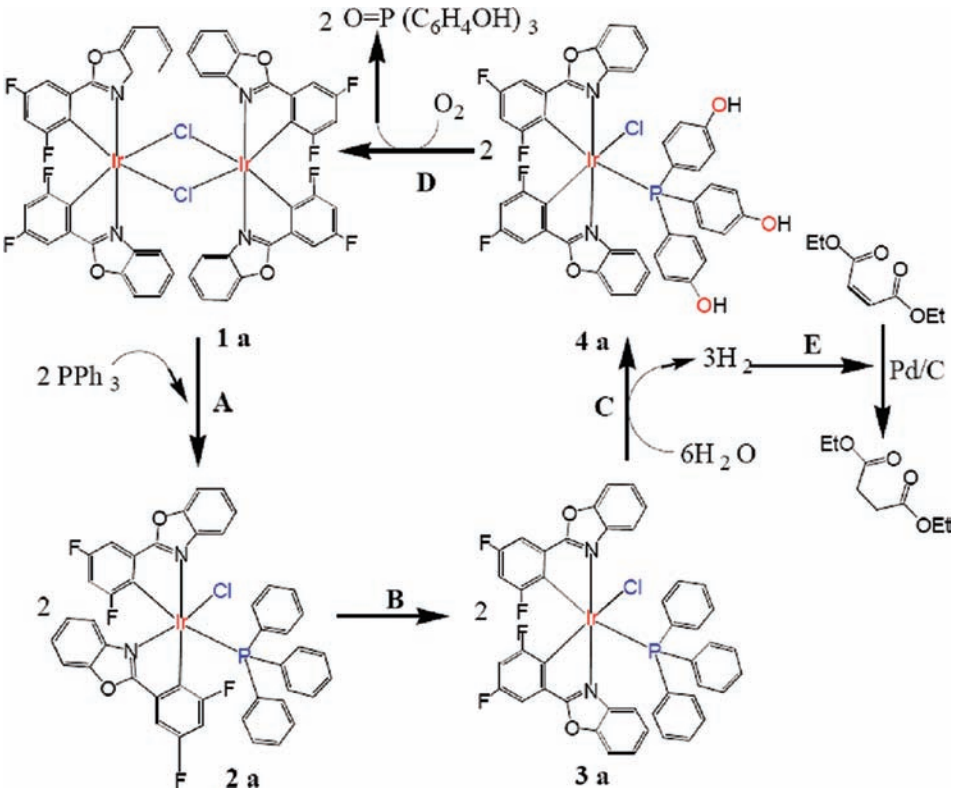

Figure 4. Catalytic cycle for water splitting to produce hydrogen.

was first formed, and then the formation of compound **3a** was observed. After 5 h, all of **1a** and **2a** were completely converted into **3a**, which implies that compound **2a** tends to convert to a more stable configuration, **3a** (Figure 4, route B, and Figure S10 and Tables S12 and S13 in the SI) with a *trans*-N−N structure possessing more reasonable bonding parameters ($\alpha = 86.33$, $\beta = 97.01$, md = 0.023, and DA = 86.8; Table 1).

The time-dependent ^{31}P NMR spectrum of **3a** in toluene-d_8 containing a trace amount of water under nitrogen at 90 °C (Figure S11 in the SI) shows that compound **3a** was gradually transformed to **4a**, $(C^\wedge N)_2Ir[P(C_6H_4OH)_3]$ ($C^\wedge N$ = 2-(3.5-difluorophenyl)benzoxazolato-N,C^2) with *trans*-N−N disposition (Figure S12 and Tables S12 and S13 in the SI), which means that the PPh$_3$ ligand of **3a** is extremely electron-deficient like that of **2a**. The phenyl rings of the PPh$_3$ group for **3a** are thus umpolung and become good electrophiles, and even a weak nucleophile, water, can attack these phenyl groups. The time-dependent electron spin resonance spectra of the degassed solution of complex **3a** in toluene at 77 and 360 K were silent, which means that a paramagnetic or radical intermediate was not involved in this reaction. On the basis of the above-mentioned information, we proposed an addition−elimination mechanism

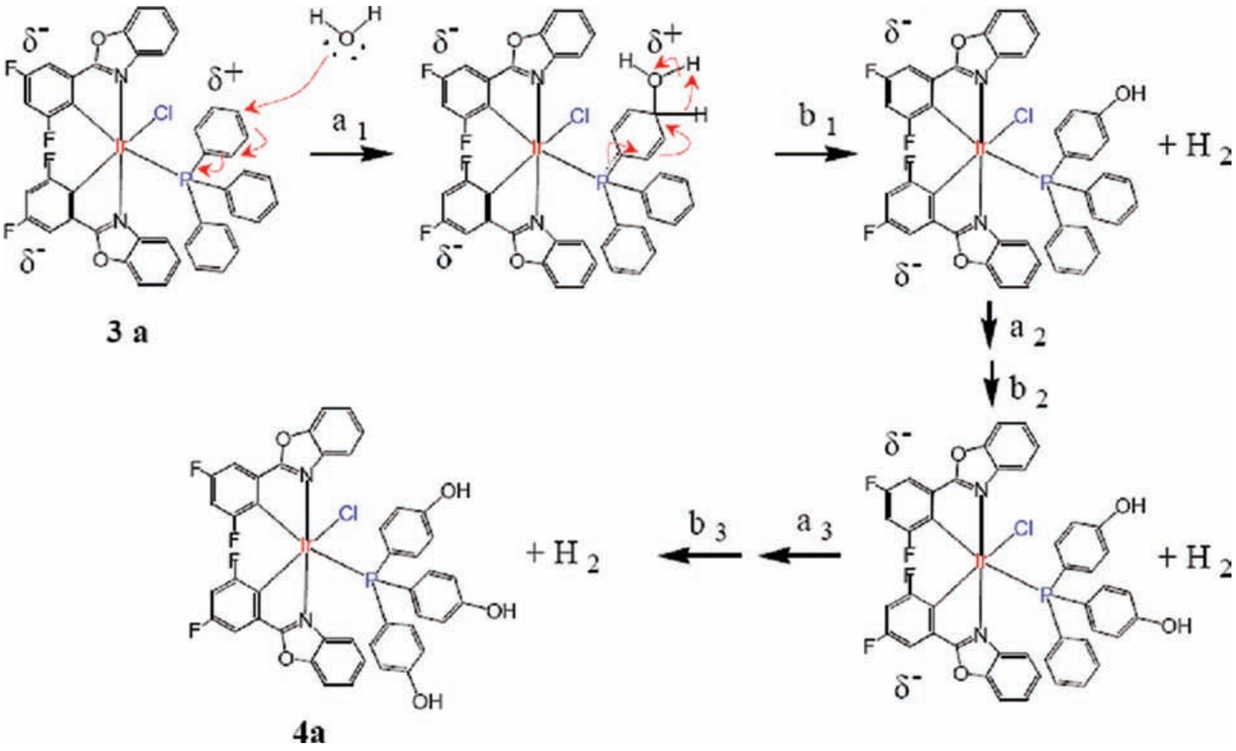

Figure 5. Addition–elimination mechanism for the reaction of **3a** with water.

to explain the nucleophilic addition of water to the phenyl rings of the PPh_3 ligand for **3a** (Figure 5). Because the cyclometalating ligands of **3a** are electron-withdrawing and sterically bulky, the nucleophlic addition of a water molecule occurs entirely at the para position of the umpolung phenyl ring and leads to dearomatization for this umpolung phenyl ring (Figure 5, step a_1). The rearomatization reaction then directs a hydride migration from the sp^3 carbon of the dearomatized system to the aryloxonium ion, followed by the formation of hydrogen and a (monohydroxophenyl)diphenylphosphine ligand (Figure 5, step b_1). Afterall, the PPh_3 ligand was transformed to (trihydroxophenyl)phosphine and the iridium complex **4a** was obtained.

The production rate of hydrogen for the above-mentioned reaction was fast and steady in the early stage (the average rate in the first 10 min was 1.8 μmol s^{-1}), and then the speed slowed when the concentration of **3a** decreased (Figure 6). The hydrogen produced could be collected by the method of water displacement (Figure S13 in the SI) and verified by consumption of diethyl maleate (Figure 4, routes C and E).

When a solution of complex **4a** in toluene/water was refluxed under an inert atmosphere of nitrogen for over 48 h, the concentration of complex **4a** remained unchanged and no product formed, which means that a water molecule would not attack the iridium center of complex **4a**. However, when this solution was exposed to air, complex **4a** quickly disappeared and an organophosphorus compound, tris(4-hydroxyphenyl)phosphine oxide (**5a**), and the starting material **1a** were obtained, which could be attributed to the oxidative addition of O_2 to complex **4a** and the reductive elimination of **5a** from the iridium center; two iridium fragments, $(C^\wedge N)_2Ir(Cl)$, combined with each other to form the starting material **1a**. The composition and structure of **5a** are identified by NMR spectroscopy, elemental analysis, and high-resolution mass spectra ($m/z = 326.0708$), and

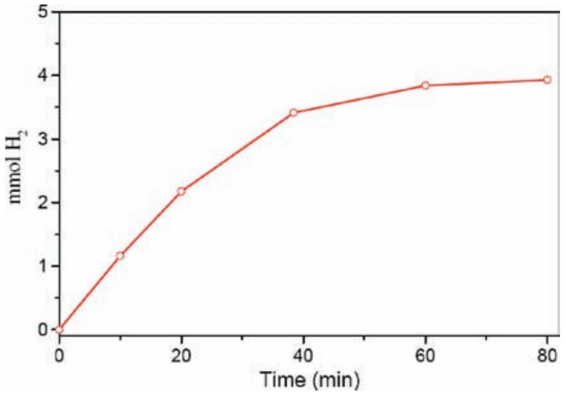

Figure 6. Plot of hydrogen production for complex **3a** dissolved in a toluene/water solution (0.03 M) at 85 °C.

the spectral data of the recovered **1a** are the same as those of compound **1a**. Therefore, a catalytic cycle (Figure 4) for the production of hydrogen and (hydroxyphenyl)phosphine was obtained.

The nucleophilic addition of water to the phenyl groups of **2b** and **2c** was not observed, which implies that a sufficient intramolecular charge separation (ICS) is needed for the umpolung of these phenyl groups, and the electron-withdrawing ability of cyclometallic ligands of **2a** could provide a suitable ICS effect for the umpolung of this aromatic system. To our best knowledge, this is the first catalytic cycle using an organometallic compound as the catalyst in a thermal water splitting system to produce hydrogen.

CONCLUSION

A new type of iridium complex was discovered that possesses umpolung phenyl rings. This umpolung aromatic system can react with water, a weak nucleophile, to produce hydrogen and (hydroxyphenyl)phosphine. The electron-withdrawing ability of cyclometalating ligands is important for the umpolung of the aromatic system of the arylphosphine ligand.

■ EXPERIMENTAL SECTION

Methods and Materials. All solvents were of analytical reagent grade and were purified according to the standard procedure.[8] 3,5-Difluorobenzoic acid was purchased from Matrix and $IrCl_3 \cdot 3H_2O$ from Seedchem Co. All other chemicals were purchased from Acros and used as received. NMR spectra were measured on a Bruker Advance-400 MHz or a Mercury 300 MHz NMR spectrometer. Elemental analyses (C, H, and N) were obtained from an Elementar Vario EL III analyzer. Mass spectra were taken with a Finnigan/Thermo Quest MAT 95XL instrument with electron impact ionization for organic compounds or fast atom bombardment for metal complexes.

X-ray Structure Determinations. The diffraction data of complexes **2a**–**2c**, **3a**, and **4a** were collected on a Bruker SMART APEX CCD diffractometer with graphite-monochromatized Mo Kα radiation ($\lambda = 0.710\,73$ Å) at 105 K for **2a** and **3a** and at 297 K for **2b**, **2c**, and **4a**. All of the calculations for structure determination were carried out using the *SHELXTL* package (version 5.1).[9] The positions of the heavy atoms, including the iridium atoms, were located by direct methods. The remaining atoms were found in a series of alternating difference Fourier maps and least-squares refinement.[10] Basic information pertaining to the crystal parameters and structure refinement is summarized in Tables S1 and S12 in the SI. Selected bond distances and angles are listed in Tables S2 and S13 in the SI.

DFT Calculations. DFT calculations were performed with the *Gaussian 03* program suite[11] at the B3LYP/LANL2DZ level to optimize the geometry structures and to calculate the molecular orbitals, dipole moment, and Mulliken charge distribution for **2a**–**2c**.

Preparation of 1a–1c. Cyclometalated iridium(III) chloro-bridged dimers (**1a**–**1c**) were synthesized according to a previous method.[12] A flask was charged with 10 mmol of iridium trichloride ($IrCl_3 \cdot 3H_2O$) and 22 mmol of an appropriate benzoxazole derivative, 2-(3,5-difluorophenyl)benzoxazole for **1a**, 2-phenylbenzoxazole for **1b**, and 2-naphthylbenzoxazole for **1c**. A solvent mixture composed of 60 mL of 2-ethoxylethanol and 20 mL of water was added to the above-mentioned flask, and the resulting solution was stirred and warmed to 100 °C for 24 h under nitrogen. After cooling to room temperature, the mixture was poured into 300 mL of pure water, and the precipitate of the cyclometalated iridium dimer was collected, washed with deionized water, and dried at 60 °C in a vacuum oven.

*Experimental Data of **1a***. Dark yellow solid. Yield: 75% ^{1}H NMR [300 MHz, DMSO-d_6, 298 K; δ (ppm)]: 8.18 (d, J = 8.1 Hz, 4H), 7.31 (dd, J = 7.6 and 2.7 Hz, 4H), 7.22–7.12 (m, 8H), 6.99 (dt, J = 7.1 and 1.5 Hz, 4H), 6.14 (dt, J = 9.6 and 2.7 Hz, 4H). ^{13}C NMR [75 MHz, $CDCl_3$, 298 K; δ (ppm)]: 174.9, 169.2, 169.1, 167.5, 167.4, 160.3, 160.2, 158.7, 158.6, 149.1, 140.8, 133.6, 133.5, 133.4, 133.3, 125.1, 124.4, 118.0, 115.3, 115.0, 110.9, 108.6, 108.4, 107.2, 107.0, 106.8, 31.8, 31.1, 22.8, 14.3. Anal. Calcd for $C_{52}H_{24}F_8Cl_2Ir_2N_4O_4$ (MW = 1376.12): C, 45.38; H, 1.76; N, 4.07. Found: C, 44.89; H, 1.70; N, 3.98. MS (FAB; m/z): 1376.0319.

*Experimental Data of **1c***. Red solid. Yield: 65% ^{1}H NMR [300 MHz, DMSO-d_6, 298 K; δ (ppm)]: 8.93 (d, J = 8.4 Hz, 2H), 8.63 (s, 2H), 8.48 (s, 2H), 8.38 (s, 2H), 8.16 (d, J = 7.5 Hz, 2H), 8.11 (d, J = 7.2 Hz, 2H), 7.93 (d, J = 7.2 Hz, 2H), 7.83–7.80 (m, 4H), 7.71–7.57 (m, 8H), 7.37 (t, J = 7.8 Hz, 2H), 7.25–7.23 (m, 4H), 7.14 (t, J = 7.5 Hz, 2H), 7.02–7.0 (m, 2H), 6.5 (d, J = 7.5 Hz, 2H), 6.37 (s, 2H). Anal. Calcd for $C_{68}H_{40}Cl_2Ir_2N_4O_4$ (MW = 1432.43): C, 57.02; H, 2.82; N, 3.91. Found: C, 56.28; H, 3.82; N, 2.85. MS (FAB; m/z): 1432.1689.

Preparation of 2a and 3a. A flask was charged with 2 mmol (2.752 g) of **1a**, 5 mmol (1.30 g) of triphenylphosphine, and 100 mL of toluene. The solution was stirred under nitrogen and warmed to 100 °C. Intermediate **2a** first formed and then transformed into **3a**; however, **2a** can be isolated and identified during the reaction. After 5 h, all of **1a** and **2a** was completely converted into **3a**, the solution was cooled to room temperature, and the reaction mixture was purified by column chromatography.

*Experimental Data of **2a***. ^{1}H NMR [300 MHz, $CDCl_3$, 298 K; δ (ppm)]: 7.22–7.33 (m, 7H), 6.99–7.07 (m, 2H), 6.63–6.86 (m, 12H), 6.36–6.48 (m, 3H), 6.02 (s, 2H), 5.56 (s, 1H). ^{13}C NMR [75 MHz, $CDCl_3$, 298 K; δ (ppm)]: 139.4, 137.8, 134.8, 133.7, 133.5, 132.2, 131.6, 129.4, 127.5, 127.4, 125.2, 124.9, 124.5, 123.5, 122.2, 121.9, 118.9, 114.9, 111.6, 111.4. ^{31}P NMR [121 MHz, $CDCl_3$, 298 K; δ (ppm)]: −12.77 (s). Anal. Calcd for $C_{44}H_{27}N_2O_2ClF_4IrP$ (MW = 950.3761): C, 55.61; H, 2.86; N, 2.95. Found: C, 54.49; H, 2.75; N, 2.84. MS (FAB; m/z): 950.1065.

*Experimental data of **3a***. Yield: 90%. ^{1}H NMR [300 MHz, $CDCl_3$, 298 K; δ (ppm)]: 7.22–7.33 (m, 7H), 6.63–7.6 (m, 23H), 6.39 (t, J = 7.5 Hz, 1H), 5.92 (q, J = 9.9 Hz, 2H). ^{13}C NMR [75 MHz, $CDCl_3$, 298 K; δ (ppm)]: 149.3, 149., 139.6, 134.6, 132.6, 131.3, 130.7, 129.7, 128.8, 127.4, 127.2, 125.3, 125.1, 124.9, 123.8, 121.0, 119.6, 118.6, 115.3, 113.9, 111.3, 110.1, 109.1, 108.8, 108.2, 107.9, 107.5, 107.2, 106.8. ^{31}P NMR [121 MHz, $CDCl_3$, 298 K; δ (ppm)]: −18.2 (s). Anal. Calcd for $C_{44}H_{27}N_2O_2ClF_4IrP$ (MW = 950.3761): C, 55.61; H, 2.86; N, 2.95. Found: C, 54.49; H, 2.75; N, 2.84. MS (FAB; m/z): 950.1065.

Preparation of 2b and 2c. A flask was charged with 5 mmol of triphenylphosphine, 100 mL of toluene, and 2 mmol of an appropriate cyclometalated iridium(III) chloro-bridged dimer, **1b** for **2b** and **1c** for **2c**. The solution was stirred under nitrogen and warmed to 100 °C for 24 h. After cooling to room temperature, the reaction mixture was purified by column chromatography.

*Experimental Data of **2b***. Yield: 85%. ^{1}H NMR [300 MHz, $CDCl_3$, 298 K; δ (ppm)]: 7.91 (d, J = 7.8 Hz, 1H), 7.77–7.79 (m, 1H), 7.70 (d, J = 8.1 Hz, 1H), 7.48–7.60 (m, 6H), 7.34–7.39 (m, 1H), 7.21 (d, J = 8.4 Hz, 1H), 7.05–7.13 (m, 5H), 6.82–7.00 (m, 12H), 6.69–6.75 (m, 1H), 6.31–6.39 (m, 1H), 6.05 (d, J = 7.8 Hz, 1H). ^{31}P NMR [121 MHz, $CDCl_3$, 298 K; δ (ppm)]: −10.13 (s). Anal. Calcd for $C_{44}H_{31}N_2O_2$-ClIrP (MW = 878.4141): C, 60.16; H, 3.56; N, 3.19. Found: C, 58.36; H, 3.43; N, 3.07. MS (FAB; m/z): 878.

*Experimental Data of **2c***. Yield: 86%. ^{1}H NMR [300 MHz, $CDCl_3$, 298 K; δ (ppm)]: 8.35 (s, 1H), 8.15 (d, J = 9 Hz, 2H), 7.84–7.87 (m, 1H), 7.77 (d, J = 8.1 Hz, 1H), 7.61–7.70 (m, 1H), 7.32–7.56 (m, 10H), 7.25–7.32 (m, 1H), 7.04–7.19 (m, 7H), 6.81–6.94 (m, 8H), 6.78 (t, J = 8.1 Hz, 1H), 6.65 (d, J = 8.1 Hz, 1H), 6.14 (d, J = 11.4 Hz, 1H). ^{31}P NMR [121 MHz, $CDCl_3$, 298 K; δ (ppm)]: −8.76 (s). Anal. Calcd for $C_{52}H_{35}N_2O_2ClIrP$ (MW = 978.5337): C, 63.83; H, 3.61; N, 2.86. Found: C, 62.23; H, 3.49; N, 2.74. MS (FAB; m/z): 978.

■ ASSOCIATED CONTENT

Ⓢ **Supporting Information.** Experimental details, analytical data, X-ray details for **2a**–**2c** and **3a**–**5a**, crystallographic information in CIF format for **2a**–**2c**, **3a**, and **4a**, tables of Cartesian coordinates, and HOMO and LUMO orbital compositions for **2a**–**2c**. This material is available free of charge via the Internet at http://pubs.acs.org.

■ AUTHOR INFORMATION

Corresponding Author

*E-mail: trchen@mail.npue.edu.tw.

ACKNOWLEDGMENT

This work was supported by the National Science Council of the Republic of China (Grant NSC 99-2113-M-153-001).

REFERENCES

(1) (a) Dickstein, J. S.; Fennie, M. W.; Norman, A. L.; Paulose, B. J.; Kozlowski, M. C. *J. Am. Chem. Soc.* **2008**, *130*, 15794–15798. (b) Nelson, A. P.; DiMagno, S. D. *J. Am. Chem. Soc.* **2000**, *122*, 8569–8570. (c) Miyake, H.; Kano, N.; Kawashima, T. *J. Am. Chem. Soc.* **2009**, *131*, 16622–16623. (d) Fischer, C.; Smith, S. W.; Powell, D. A.; Fu, C. G. *J. Am. Chem. Soc.* **2006**, *128*, 1472–1473. (e) Tan, Y.; Hartwige, J. F. *J. Am. Chem. Soc.* **2010**, *132*, 3676–3677. (f) Mattson, A. E.; Scheidt, K. A. *J. Am. Chem. Soc.* **2007**, *129*, 4508–4509. (g) Wang, W.; Zhang, T.; Shi, M. *Organometallics* **2009**, *28*, 2640–2642. (h) Araki, S.; Kameda, K.; Tanaka, J.; Hirashita, T.; Yamamura, H.; Kawai, M. *J. Org. Chem.* **2001**, *66*, 7919–7921. (i) Garker, T. J.; Jarvo, E. R. *J. Am. Chem. Soc.* **2009**, *131*, 15598–15599. (j) Hatcher, J. M.; Coltart, D. M. *J. Am. Chem. Soc.* **2010**, *132*, 4546–4547.

(2) Brown, D. A.; Fitzpatrick, N. J.; Glass, W. K.; Taylor, T. H. *Organometallics* **1986**, *5*, 158–162.

(3) (a) Eisenberg, R. *J. Am. Chem. Soc.* **2008**, *130*, 5056–5058. (b) Yoshida, H.; Hirao, K.; Nishimoto, J.-I.; Shimura, K.; Kato, S.; Itoh, H.; Hattori, T. *J. Phys. Chem. C* **2008**, *112*, 5542–5551.

(4) (a) Elvington, M.; Brown, J.; Arachchige, S. M.; Brewer, K. J. *J. Am. Chem. Soc.* **2007**, *129*, 10644–10645. (b) McCormick, T. M.; Calitree, B. D.; Orchard, A.; Kraut, N. D.; Bright, F. V.; Detty, M. R.; Eisenberg, R. *J. Am. Chem. Soc.* **2010**, *132*, 15480–15483. (c) Du, P.; Schneider, J.; Luo, G.; Brennessel, W. W.; Eisenberg, R. *Inorg. Chem.* **2009**, *48*, 4952–4962. (d) Ison, E. A.; Corbin, R. A.; Abu-Omar, M. M. *J. Am. Chem. Soc.* **2005**, *127*, 11938–11939. (e) Du, P.; Knowles, K.; Eisenberg, R. *J. Am. Chem. Soc.* **2008**, *130*, 12576–12577.

(5) (a) Chen, T.-R. *J. Organomet. Chem.* **2008**, *693*, 3117–3130. (b) Lee, H.-P.; Hsu, Y.-F.; Chen, T.-R.; Chen, J.-D.; Chen, K. H.-C.; Wang, J.-C. *Inorg. Chem.* **2009**, *48*, 1263–1265. (c) Chen, T.-R.; Lee, H.-P.; Chen, J.-D.; Chen, K. H.-C. *Dalton Trans.* **2010**, *39*, 9458–9461.

(6) (a) Ariafard, A.; Brookes, N. J.; Stranger, R.; Yates, B. F. *J. Am. Chem. Soc.* **2008**, *130*, 11928–11938. (b) Um, J. M.; Gutierrez, O.; Schoenebeck, F.; Houk, K. N.; MacMillan, D. W. C. *J. Am. Chem. Soc.* **2010**, *132*, 6001–6005.

(7) (a) Atanasov, M.; Comba, P.; Daul, C. A. *J. Phys. Chem. A* **2006**, *110*, 13332–13340. (b) van der Vlugt, J. I.; Fioroni, M.; Ackerstaff, J.; Hanssen, R. W. J. M.; Mills, A. M.; Spek, A. L.; Meetsma, A.; Abbenhuis, H. C. L.; Vogt, D. *Organometallics* **2003**, *22*, 5297–5306. (c) Buda, B. E. F.; Gribnau, M. C. M.; Baerends, E. J. *J. Am. Chem. Soc.* **2004**, *126*, 4355–4365. (d) Roncaroli, F.; Ruggiero, M. E.; Franco, D. W.; Estiú, G. L.; Olabe, J. A. *Inorg. Chem.* **2002**, *41*, 5760–5769.

(8) Perrin, D. D.; Armarego., W. L. F. *Purification of Laboratory Chemicals*, 3rd ed.; Pergamon Press: New York, 1988.

(9) (a) *XSCANS*, release 2.1; Siemens Energy & Automation, Inc.: Madison, WI, 1995. (b) *SMART/SAINT/ASTRO*, release 4.03; Siemens Energy & Automation, Inc.: Madison, WI, 1995.

(10) *SHELXTL 5.10*; Bruker Analytical X-ray Instruments Inc.: Karlsruche, Germany, 1997.

(11) Frisch, M. J.; Trucks, G. W.; Schlegel, H. B.; Scuseria, G. E.; Robb, M. A.; Cheeseman, J. R.; Montgomery, J. A., Jr.; Vreven, T.; Kudin, K. N.; Burant, J. C.; Millam, J. M.; Iyengar, S. S.; Tomasi, J.; Barone, V.; Mennucci, B.; Cossi, M.; Scalmani, G.; Rega, N.; Petersson, G. A.; Nakatsuji, H.; Hada, M.; Ehara, M.; Toyota, K.; Fukuda, R.; Hasegawa, J.; Ishida, M.; Nakajima, T.; Honda, Y.; Kitao, O.; Nakai, H.; Klene, M.; Li, X.; Knox, J. E.; Hratchian, H. P.; Cross, J. B.; Adamo, C.; Jaramillo, J.; Omperts, R.; Stratmann, R. E.; Yazyev, O.; Austin, A. J.; Cammi, R.; Pomelli, C.; Ochterski, J. W.; Ayala, P. Y.; Morokuma, K.; Voth, G. A.; Salvador, P.; Dannenberg, J. J.; Zakrzewski, V. G.; Dapprich, S.; Daniels, A. D.; Strain, M. C.; Farkas, O.; Malick, D. K.; Rabuck, A. D.; Raghavachari, K.; Foresman, J. B.; Ortiz, J. V.; Cui, Q.; Baboul, A. G.; Clifford, S.; Cioslowski, J.; Stefanov, B. B.; Liu, G.; ; Liashenko, A.; Piskorz, P.; Komaromi, I.; Martin, R. L.; Fox, D. J.; Keith, T.; Al-Laham, M. A.; Peng, C. Y.; Nanayakkara, A.; Challacombe, M.; Gill, P. M. W.; Johnson, B.; Chen, W.; Wong, M. W.; Gonzalez, C.; Pople, A. *Gaussian 03*, revision B.04; Gaussian, Inc.: Pittsburgh, PA, 2003.

(12) Wu, L.-L.; Yang, C.-H.; Sun, I.-W.; Chu, S.-Y.; Kao, P.-C.; Cao, Y.; Huang, H.-H. *Organometallics* **2007**, *26*, 2017–2023.